

Real-Time Maximum Power Point Tracking Algorithm (MPPT) Control of PV Systems Using Fuzzy Logic Enhanced with Adaptive Dove Swarm Optimization (ADSO) on a dSPACE Platform

Tamilselvan R

Assistant Professor

Department of Electrical Engineering

Annamalai University -608002

Article Info

Page Number:1 - 19

Publication Issue:

Vol 64 No. 1 (2015)

Abstract: Photovoltaic (PV) system has emerged as a reliable and resilient energy source due to their emission-free operation and minimal maintenance requirements. Maximum power point tracking (MPPT) approaches are required to ensure effective power extraction in various types of environmental conditions. This study presents a real-time MPPT control strategy with a boost converter for the dSPACE-implemented commercial PV panel. A fuzzy logic controller (FLC) is designed to work MPPT, and its performance is benchmark against the traditional incremental conduction (Inccond) algorithm. To further increase the tracking accuracy and dynamic reaction, the fuzzy logic controller is hybridized with the adaptive dove swarm optimization (ADSO) algorithm. The ADSO algorithm allows adaptive tuning of fuzzy membership features and rule sets based totally on real-time irradiance and temperature variations, effectively enhancing convergence velocity and robustness. Results from experiments indicate that the counselled Hybrid fuzzy-ADSO technique drastically outperforms IncCond in phrases of consistent-noise oscillation, response time and overshoot reduction. These results verify that the counselled technique for excessive efficiency is successful, actual-time MPPT control in PV structures.

Article History:

Article Received: 15 August 2015

Revised: 24 September 2015

Accepted: 18 October 2015

Keywords: Photovoltaic (PV) Systems, Maximum Power Point Tracking (MPPT), Fuzzy Logic Controller (FLC), Adaptive Dove Swarm Optimization (ADSO), dSPACE Platform, Boost Converter, Hybrid Intelligent Control, Renewable Energy, Real-Time Control, Soft Computing Techniques

I. INTRODUCTION

In recent years, growing concerns about global warming and increasing crude oil prices have driven countries around the world to significantly invest in the investigation and advancement of technology for renewable energy. Among these, solar energy has emerged as a major focus, with its applications ranging from powering small consumer devices to supporting large-scale solar power plants. However, improving a system to get the most power possible

photovoltaic (PGS) has been a major area of emphasis owing to the relatively poor energy conversion efficiency of PGS and the greater cost of solar power compared to thermal or nuclear energy. Shows are not linear of a solar cell. And vary with the intensity of sunlight and changes in the surrounding temperature, produces a different current (I V) characteristic. As a result, it is necessary to adjust the operating point (OP) of a photovoltaic generation system (PGS) to operate solar cells on their highest efficiency. This process is known as maximum power point tracking (MPPT) [1,2,3].

The most common MPPT approach in commercial photovoltaic panel production systems is disturbances and inspection (P&O) [4]. This control is operated by analysing changes in power generation between the current and previous systems states to accommodate the command. Therefore, it is important to choose a suitable disturbance step. A large disturbance steps allow the system to reach the maximum power point (MPP) and stabilize more rapidly, but this results in over -power loss due to the size of disturbances. In contrast, because it slows down the system's capacity to monitor the maximum power point, using a small disturbance step can reduce the loss of power related to the disturbance process. This situation is often referred to as accuracy versus tracking speed trade-off [5,6,7]. This trade-off usually affects MPPT methods that use a certain-step shape. To address this issue, many researchers have developed different variable phase size MPPT strategies. Increasing disturbances in the ratio of the distance between the operational point (OP) and MPP is the original concept behind the variable phase size MPPT. When the OP is ahead of the OP MPP on increasing the tracking speed of the system, an additional disturbance steps are required. To enhance the ability to achieve and maintain a stable operating status, a small disturbance step is used when OP comes to MPP [8,9,10]. The variable phase MPPT algorithms discussed in earlier research mainly determine the disturbance steps based on the OP in the power-voltage (P-V) curve of solar cells. Since the characteristic decrease of solar cells may vary depending on the operating environment, determining a disturbance phase size suitable for each type of operating position is a significant problem in the corresponding variable phase MPPT. An alternative method for management of nonlinear systems is to use fuzzy logic controller (FLC)-based techniques. These methods provide strong performance without the need for accurate system parameters or complex mathematical modelling. As a result, FLC-based MPPT techniques have attracted significant attention as a promising field of research [11].

The increasing demand for sustainable and clean energy has greatly increased the use of photovoltaic (PV) systems. These systems offer an effective option to traditional energy sources, as they generate electricity directly from solar without producing harmful emissions. Additionally, the shortage of transferring components in PV panels reduces mechanical put on and upkeep charges, making them perfect for long-term deployment in both city and remote environments. PV systems' overall performance is greatly inspired by means of external conditions like solar depth, temperature, and shading. As an effect of these variables, the PV array's running factor fluctuates, generating uneven energy production. To get around this trouble, the machine's working factor is constantly changed the use of MPPT algorithms, which ensure device operation close to MPP.

Based on their convenience of use and reasonable overall performance, traditional MPPT techniques like Perturb and Observe (P&O) and Incremental Conductance (IncCond) had been frequently hired. The inconsistency around MPP is one of the disadvantages of these methods, delayed response during rapidly changing conditions, and partially trekking into a partially shaded environment.

To remove these boundaries, a soft computing approach, especially fuzzy logic controllers (FLC), have gained popularity in MPPT applications. An accurate mathematical details of the PV system are not required for FLCs because they are naturally flexible. Their rule-based decision-making ability allows for better performance in smooth control tasks and dynamic conditions. However, traditional FLCs usually use static membership functions and rules sets, which can limit adaptability and adaptation in diverse environmental conditions.

To deal with these challenges, this research proposes a hybrid intelligent MPPT control method that combines fuzzy logic with adaptive dove swarm adaptation (ADSO). The forging method serves as an inspiration to the ADSO pattern of the metaheuristic algorithm of pigeons and operates on a population-based approach. It dynamically adjusts its internal parameters in reaction to environmental changes, correctly balancing exploration and exploitation. This adaptability makes it nicely-appropriate for real-time manage programs wherein both fast convergence and specific tracking are critical.

This work conducts a commercial photovoltaic panel that coupled to a boost converter in real time using a DSPAS platform. The proposed fuzzy logic -ADSO hybrid controller is evaluated and unlike the traditional approach to incremental conduction. Reaction time, steady-set oscillation, and overshoot decrease is greatly enhanced by the proposed method, according to experimental data, the practical PV system valid its effectiveness for real-time MPPT in the practical PV system.

The following is the structure of paper: Section 2 examines relevant research and MPPT methods. Section 3 underlines the design and system architecture of the suggested fuzzy-fund controller. Section 4 describes the setup and results of the experiment. Section 5 provides a show assessment. Section 6 brings the task to a conclusion and identifies possible directions for further studies.

II. RELATED WORKS

A novel Maximum Power Point Tracking (MPPT) method primarily based on Ant Colony Optimization (ACO) is a first-rate contribution designed for photovoltaic (PV) system working in in part shaded environment [12]. Conventional MPPT techniques war to deal with many local maxima as a result of shade. Adapting the ACO set of rules to efficaciously navigate those complicated terrains discovered the actual worldwide maximum power factor. The performance of the system was evaluated entirely using simulation, and the findings indicated that in terms of tracking accuracy and convergence speed, it was more capable than traditional methods such as P&O and incremental conduction. Results show how effectively ACO algorithm can increase energy production in challenging the actual PV configuration.

In terms of wind energy, [13] presented a better real-time non-linear model Predictive Control (NMPC) method for wind turbines using a splutter-interpolated aerodynamic coefficient. This approach aimed to optimize turbine blade control for best economic efficiency under very changing wind conditions. By using spline interpolation, the model more accurately reflected nonlinear aerodynamic properties, which resulted in more fluid and responsive control actions. When evaluated with real-time simulations, the method revealed significant increases in operational stability and power generation consistency, indicating that it may be used in large wind farms.

Particularly for PV systems operating in partially shaded situations, an MPPT approach based on particle swarm optimization (PSO) was developed in [14]. Because it was clear that traditional MPPT algorithms are prone to local maxima, especially in the presence of non-uniform irradiance, global searches across the power-voltage curve were performed using the PSO method. The method's enhanced ability to avoid local traps and reliably converge to the true maximum power point was confirmed by means of MATLAB simulations. In contrast to conventional MPPT methods, the PSO-based system demonstrated more rapid convergence and improved energy harvesting efficiency under complex shading conditions.

An [15] suggested improved PSO-based method advanced the area of metaheuristic MPPT algorithms and assisted to lower steady-state oscillations. Though they sometimes create small but lasting oscillations that reduce system efficiency, conventional PSO methods are excellent at monitoring the maximum power point. In this study, the inertia weight and acceleration coefficients were dynamically changed to stabilize the particle movements around the MPP. The system was evaluated under conditions of changing irradiance using MATLAB simulations. The results showed significant improvements in convergence stability and power extraction consistency, hence qualifying the system as an excellent option for high-performance PV control.

Solar PV systems were given an MPPT controller constructed in [16] using the Adaptive Neuro-Fuzzy Inference System (ANFIS). The method allows it to react dynamically to temperature and sun irradiance variations by integrating the learning capability of neural networks with the decision-making framework of fuzzy logic. A DC-DC converter's optimal duty cycle is determined by the controller in order to maximize power output. According to simulation results validated using MATLAB/Simulink, especially in environments with fast changing conditions, the ANFIS-based MPPT controller outperformed traditional methods in terms of reaction time and tracking accuracy.

Based on artificial neural networks (ANNs), a novel MPPT algorithm was established in [17] to increase the tracking speed and adaptability of PV systems under many environmental conditions. Using trained neural networks, this method directly predicted the MPP from real-time input variables like voltage and irradiance, therefore contrasting with deterministic MPPT approaches. Developed for use in embedded devices, the approach was evaluated by thorough simulations. The results indicated that, particularly in cases of variable irradiance, the ANN-based method beat conventional MPPT strategies in terms of speed and accuracy.

In the structure of [18], many MPPT strategies for PV systems including P&O, INC, and PSOWere evaluated. Their performance under varying temperature and irradiance was the main focus of the study, which used MATLAB/Simulink simulations. PSO fared better in dynamic contexts than P&O and INC, despite the fact that both are straightforward and efficient in stable settings, according to the results. Better energy efficiency and worldwide tracking were provided by PSO. But the computational effort was higher. For the best PV performance, our paper emphasized the significance of algorithm selection.

Numerous MPPT strategies have been explored to enhance PV performance, ranging from classical methods (P&O, IncCond) to intelligent techniques such as Artificial Neural Networks (ANN), Genetic Algorithms (GA), and Particle Swarm Optimization (PSO). Recent literature shows a growing interest in hybrid systems, where optimization algorithms enhance the adaptability of fuzzy logic and neural systems.

Adaptive metaheuristic algorithms like ADSO offer advantages in dynamic parameter tuning and convergence stability. However, few studies have successfully applied them in real-time control environments. This research addresses that gap by integrating ADSO within an FLC framework for real-time MPPT on a dSPACE system.

III. PROPOSED METHODOLOGY

The suggested setup comprises a photovoltaic module combined with a boost converter whose duty cycle is regulated by a hybrid controller implemented on a dSPACE real-time platform. The MPPT algorithm utilizes fuzzy logic combined with ADSO to guarantee efficient and consistent monitoring of the optimum power point under different sun circumstances. The flow of the proposed methodology is illustrated in Figure 1.

Detailed Flow Diagram of Fuzzy-ADSO-Based MPPT Methodology

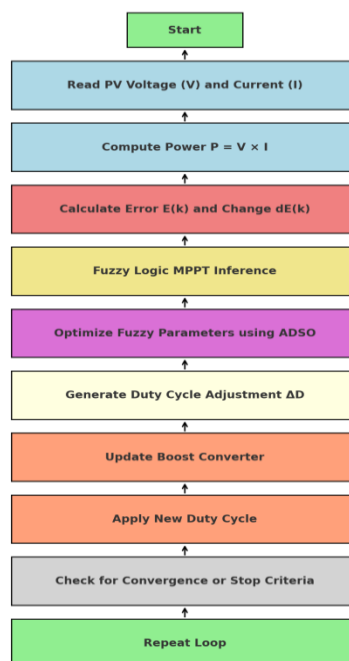
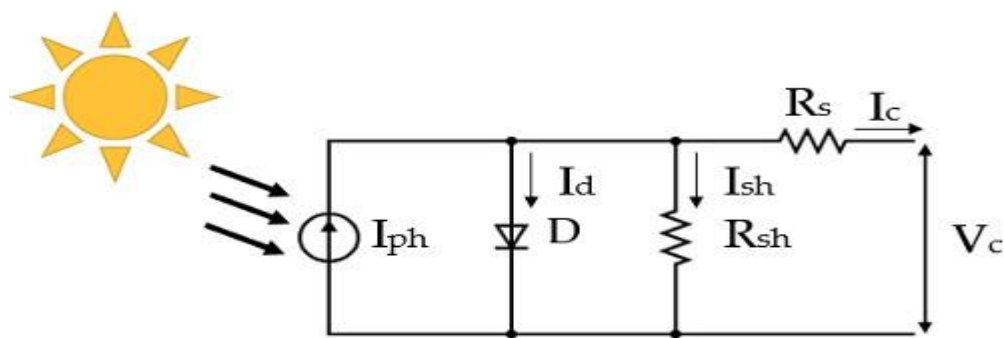


Figure 1: Flow Diagram of Fuzzy-ADSO based MPPT**3.1. PV Model**

The research used a single-diode model because of its accuracy and ease of use. As shown in Figure 2, this method simulates the PV in an electric circuit as a DC source. As a result of solar radiation, the PV produces a current I_{ph} . The diode's current leakage at the p-n junction is represented by I_{sh} , while the resistance across the PV is shown by R_s . Two other resistances are also taken into consideration. The latter reduces the maximum power output of the system.

**Figure 2. PV Model**

Equation (1), where I_{sh} and I_c are defined using the following equations, is given using Kirchhoff's current law:

$$I_c = I_{ph} - I_d - I_{sh} \quad (1)$$

$$I_c = I_{ph} - I_o \left(e^{\frac{q(V + R_s I_c)}{a k T_c}} - 1 \right) - \frac{V + R_s I_c}{R_{sh}} \quad (2)$$

The operating temperature, the Boltzmann constant, the elementary charge, and the reverse saturation current are denoted by T_c , K , q , and I_o , respectively. Equation (3), where G/G_{SRC} represents the connection between the radiance under standard rating conditions (SRCs) and the actual solar radiation, also expresses the current that the PV produces. At SRC, T_{ref} is the PV temperature and $I_{sc_{ref}}$ is the PV's short-circuit current. One component of the short-circuit current's thermal factor is kI_{ref} .

$$I_{ph} = \frac{G}{G_{ref}} \left(I_{sc_{ref}} + K_{I_{ref}} (T - T_{ref}) \right) \quad (3)$$

Equation (4) determines the output current (I_m) and voltage (V_m) of the whole PV panel, which is constructed in parallel with numerous components (N_p) and series (N_s). Thus, using the above formulas, the PVG's output current may be expressed as follows.

$$I_m = N_p I_c \quad (4)$$

$$V_m = N_s V_c \quad (5)$$

$$I_c = I_{ph} N_p - N_p I_o \left(e^{\frac{q(V+R_s I_c)}{aKT_c}} - 1 \right) - N_p \frac{V+R_s I_c}{R_{sh}} \quad (6)$$

3.2. Incremental Conductance

The IncCond tracking algorithm is popular because of its efficiency and accuracy, compared to the P&O algorithm [19]. By assessing the voltage and current conditions and implementing increment/decrement modifications, it regulates the power converter's duty cycle, D , as shown in Figure 3. The authors of [20] used an almost controlled step size in their experimental design and implementation of this approach. In addition to causing soft power oscillations in steady state, a duty cycle with a small step-size value also results in a slow dynamic response that is sensitive to external disturbances. Increasing the step size has the opposite effect, causing excessive power fluctuation in a steady state. Although the results in [20] indicated satisfactory tracking precision, the lack of evaluation under external disturbances calls its robustness into question. In fact, most traditional MPPT algorithms use a fixed step size and therefore cannot deliver both rapid response and high steady-state accuracy at the same time. A variable step size one that decreases the perturbation magnitude as the operating point nears the target is necessary to achieve both fast dynamics and precise convergence.

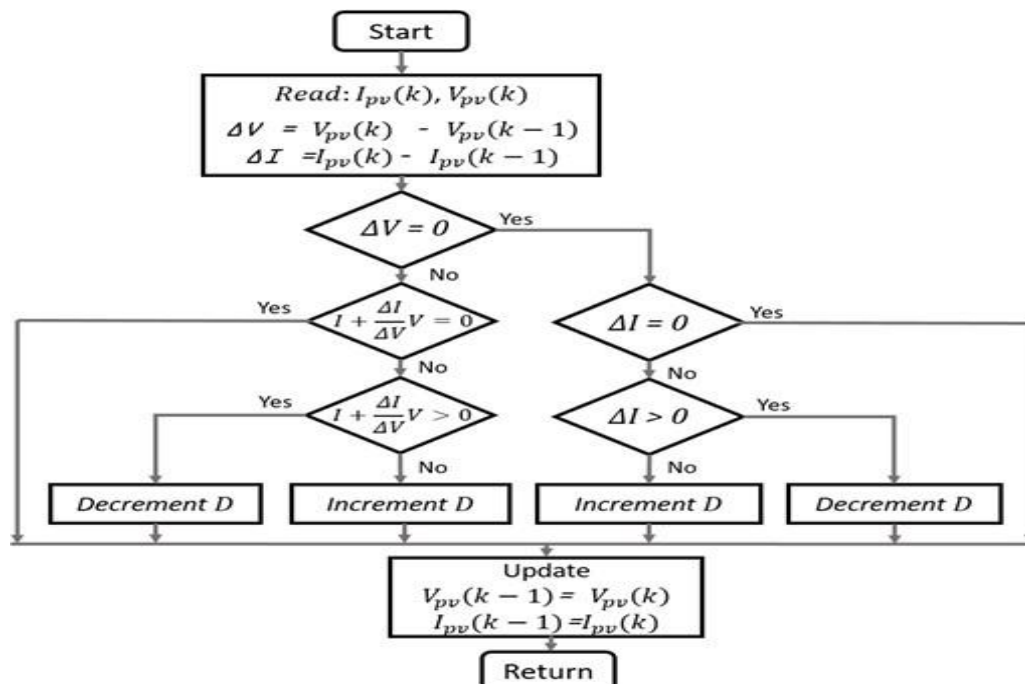


Figure 3: Flowchart of IncCond algorithm

3.3. Hybrid Fuzzy-ADSO controller

In this case, the MPPT algorithm incorporates fuzzy logic combined with ADSO to provide effective and dependable tracking of the largest power point under variable conditions solar environments.

Fuzzy-ADSO Controller Overview

To ensure effective and reliable tracking of the maximum power point under changing solar circumstances, the MPPT algorithm is based on fuzzy logic supplemented with ADSO. The fuzzy logic controller provides a human-experience-inspired, model-free control system that infers the duty cycle adjustment required for the boost converter. ADSO then fine-tunes the fuzzy rules and membership functions for optimal decision-making in changing environments.

i. Fuzzy Logic Control

An intelligent method to assess a PV system's maximum operational power point is to employ fuzzy logic control (FLC)-based MPPT algorithm. Using the system's mathematical model instead, it depends on human experience. Therefore, the proposed tracking method is developed using an adaptive, step-by-step search approach. Table 1 provides a summary of the MPP search rules, which are derived from the slope of the power–voltage curve ($P_{pv} - V_{pv}$).

Table 1: MPP Search Rules

Case	ΔP	ΔV	Research Direction	Duty Ratio
1	+	+	Right direction	$D(k) = D(k-1) - \Delta D$
2	+	-	Right direction	$D(k) = D(k-1) + \Delta D$
3	-	-	Wrong direction	$D(k) = D(k-1) - \Delta D$
4	-	+	Wrong direction	$D(k) = D(k-1) + \Delta D$

The main components are fuzzification, inference, and defuzzification FLC control system, which is seen in Figure 4. The inputs, V and P, as stated in Equations (7) and (8), are transformed into fuzzy variables by the first component.

$$\Delta V = V_{pv}(k) - V_{pv}(k-1) \quad (7)$$

$$\Delta P = P_{pv}(k) - P_{pv}(k-1) \quad (8)$$

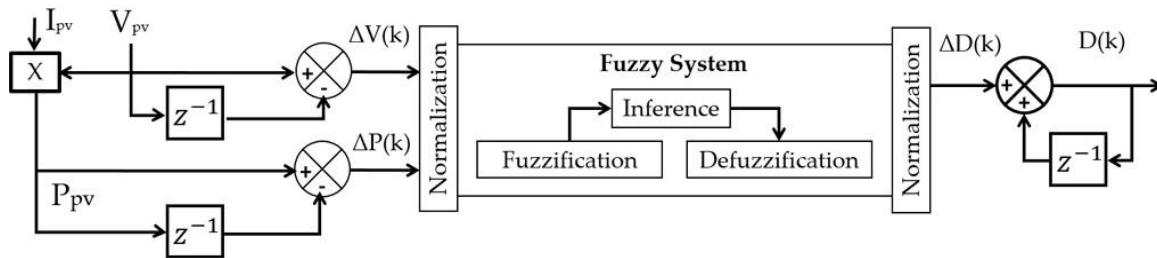


Figure 4: FLC control structure

The membership rules, which interpret the user's main logic, make up the second functional block. Table 5 lists 25 fuzzy language rules for 25 distinct situations. This table shows negative large, medium, small, zero, positive small, medium, and significant as NB, NM, NS, Z, PS, PM, and PB. The two examples that follow show how if-then statements were used to create these rules:

- If(ΔV is NS) and (ΔP is Z) then (ΔD is NS);
- If(ΔV is PB) and (ΔP is PS) then (ΔD is PM).

The third functional block, "defuzzification," is responsible for converting the inference block's verbal rules into precise numerical values. The Matlab software's fuzzy toolbox was used to setup and create the input and output membership functions.

ii. Adaptive Dove Swarm Optimization (IDSO)

ADSO optimizes the fuzzy controller by tuning the shape, width, and position of membership functions and weighting rules. Each dove represents a candidate fuzzy parameter configuration. The swarm intelligence of doves (or other birds) served as the inspiration for this metaheuristic optimization method. Does not rely on gradient information directly. Examines the parameter space using a population (swarm) of potential solutions (sets of parameters). Balances exploration and exploitation by updating positions based on swarm behavior, aiming to minimize a given loss function.

A novel optimization technique has been developed according to doves' foraging patterns. In this approach, the term $f(W)$ represents the objective function. Each data pattern, W , in the dataset is thought of as a place with crumbs, and $f(W)$ is the amount. Crumb-rich regions will be the best candidates. Figure 5 shows the DSO algorithm flowchart.

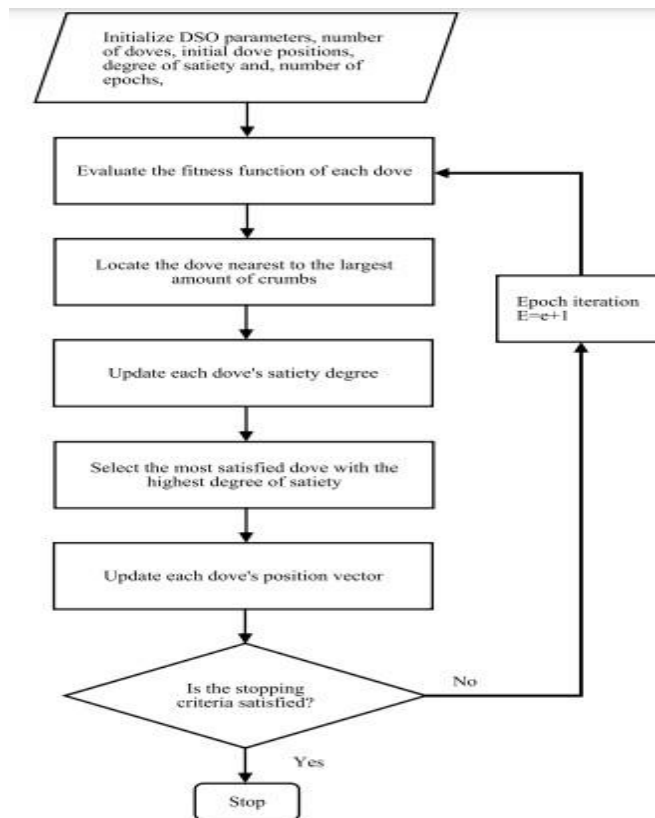


Figure 5: Flowchart of DSO

Step1: Determine the number of doves and place them within the solution space. Let the number of doves be predetermined as N . These doves can be randomly positioned within the space, but we recommend distributing them uniformly across a rectangular area.

Step2: Set the degree of satiety, s_d^e , if $e = 0$, then assume $d = 1, \dots, N$ and epochs = 0. It's possible to initialize the position vector $W_d \in R^M$ of dove d using two techniques. Initializing W_d randomly over the solution space is the most basic method. Initializing the lattice initialized technique is the alternative. The following are the steps:

Two effective weight vector initialization methods may accelerate up topologically ordered feature map training. We provide a method created especially for the algorithm based on these initiation strategies. This technique determines the parameter space's smallest hyper-rectangle, which contains all of the possible parameter values, be denoted as $[l_1, u_1], \dots, [l_M, u_M]$ where l_a and u_a symbolize the a -dimension's lower and upper constraints in the solution space. The n -dimensional hyper-rectangle is compressed into a 2-dimensional plane fundamental idea behind the suggested initialization technique, enabling a two-dimensional network to traverse the solution space. For clarity, rectangular cells are indexed from 1 to $A \times B$ using i and j . The steps are summarized:

Step 1: Cell initialization on the four corners: The network's four corners' weight vectors are set to (10).

$$w_{1,1} = (l_1, l_2, \dots, l_M)^T \quad (10)$$

$$w_{A,B} = (u_1, u_2, \dots, u_M)^T$$

$$w_{1,B} = \left(l_1, l_2, \dots, l_{\lfloor \frac{M}{2} \rfloor}, u_{\lfloor \frac{M}{2} \rfloor + 1}, \dots, u_M \right)^T$$

$$w_{A,1} = \left(u_1, u_2, \dots, u_{\lfloor \frac{M}{2} \rfloor}, l_{\lfloor \frac{M}{2} \rfloor + 1}, \dots, l_M \right)^T$$

Step 2: Cell initialization on the four edges: In accordance with (11) we initialize the value of the cells on the four edges:

$$w_{1,j} = \frac{w_{1,B} - w_{1,1}}{B-1} (j-1) + w_{1,1} \quad (11)$$

$$= \frac{j-1}{B-1} w_{1,B} + \frac{B-j}{B-1} w_{1,1} \quad \text{for } j=2, \dots, B-1$$

$$w_{A,j} = \frac{w_{A,B} - w_{A,1}}{B-1} (j-1) + w_{A,1}$$

$$= \frac{j-1}{B-1} w_{A,B} + \frac{B-j}{B-1} w_{A,1} \quad \text{for } j=2, \dots, B-1$$

$$w_{i,1} = \frac{w_{A,1} - w_{1,1}}{A-1} (i-1) + w_{1,1}$$

$$= \frac{i-1}{A-1} w_{A,1} + \frac{A-i}{A-1} w_{1,1} \quad \text{for } i=2, \dots, A-1$$

$$w_{i,B} = \frac{w_{A,B} - w_{1,B}}{A-1} (i-1) + w_{1,B}$$

$$= \frac{i-1}{A-1} w_{A,B} + \frac{B-i}{B-1} w_{1,B} \quad \text{for } i=2, \dots, A-1$$

Step 3: The remaining cells are initialized by initializing the weight vectors of the four neurons present in the network's corners.

The remaining neurons are initialized top-down and left-right. This pseudo-code describes the remaining neuron initialization procedure.

Begin

For j from 2 to B-1

Begin

For i from 2 to A-1

Begin (3), shown on the next page's bottom

End;

End;

End;

$$\begin{aligned}
 w_{i,j} &= \frac{w_{A,j} - w_{1,j}}{A-1} (i-1) + w_{1,j} = \frac{i-1}{A-1} w_{A,j} + \frac{A-i}{A-1} w_{1,j} \\
 &= \frac{i-1}{A-1} \left(\frac{j-1}{B-1} w_{A,B} + \frac{B-j}{B-1} w_{A,1} \right) + \frac{A-i}{A-1} \left(\frac{j-1}{B-1} w_{1,B} + \frac{B-j}{B-1} w_{1,1} \right) \\
 &= \frac{((j-1)(i-1)w_{A,B} + (j-1)(A-i)w_{1,B} + (B-j)(i-1)w_{A,1} + (B-j)(A-i)w_{1,1})}{(B-1)(A-1)}
 \end{aligned} \tag{12}$$

We select various sizes and assess the outcomes. The number of winning neurons and the difference value for training evaluation. Learning starts at 0.1 and decreases.

$$\eta(n) = \eta_0 \times \left(1 - \frac{t}{T}\right) = 0.1 \left(1 - \frac{t}{100}\right) \tag{13}$$

with η_0 representing the starting learning rate and t , which stands for the number of iterations.

Step 3: Number of crumbs at d th dove's position at period, compute the fitness function of all doves, $f(w_j^e), j = 1, \dots, N$.

Step 4: At epoch e , use the maximum criteria to identify the dove d_j^e most crumbs-near:

$$d_j^e = \arg \max \{f(w_j^e)\}, \text{ for } j = 1, \dots, N \tag{14}$$

Step 5: Update each dove's satiety using this equation:

$$S_j^e = \lambda S_j^{e-1} + e^{(f(w_j) - f(w_{d_j^e}))}, \text{ for } j = 1, \dots, N \tag{15}$$

Step 6: Use the following maximal standards for selecting the dove with the highest level of satiety, d_s^e :

$$d_s^e = \arg \max_{1 \leq j \leq N} \{S_j^e\}, \text{ for } j = 1, \dots, N \tag{16}$$

The dove selected by (17) to be the model for other doves in the flock to follow is d_s , who is the one demonstrating the best foraging performance.

Step7: Use the following maximum standards to update the position vector for each dove:

$$w_j^{e+1} = w_j^e + \eta \beta_j^e (w_{d_s^e}^e - w_j^e) \tag{17}$$

Where

$$\beta_j^e = \left(\frac{S_{d_s^e}^e - S_j^e}{S_{d_s^e}^e} \right) \left(1 - \frac{\|w_j^e - w_{d_s^e}^e\|}{\max \text{Distance}} \right)$$

$$\max \text{Distance} : \max_{1 \leq j \leq N} \|w_j - w_i\|$$

The parameter η is the learning rate for updates to the dove position vector. Next, updating Equations (8)-(10) are described in detail.

Step 8: To ensure that the terminate condition is satisfied, go to step 3 and by one ($e = e + 1$) to increase the number of epochs. The following is the concluding condition.

$$|f_{d_s}^e - T(e)| \leq \text{error} \leq \text{the set max epoch} \quad (18)$$

Where N_d the data set has N doves, e epochs, and data points., the dove swarm optimization method has an order of complexity of $O(NN_d e)$. If (5) and (6) are the best ways of determining the minimum (w_j^e), then the optimization is the limited standards, and they may be modified to (19) and (20) accordingly.

$$d_j^e = \arg \min \{f(w_j^e)\}, \text{ for } j = 1, \dots, N \quad (19)$$

$$S_j^e = \begin{cases} \lambda S_j^{e-1} + e^{(f(w_j) - f(w_{d_s}))}, & \text{if } f(w_{d_s}) \neq 0 \\ \lambda S_j^{e-1} + 1, & \text{if } f(w_{d_s}) = 0 \end{cases} \quad (20)$$

For $j=1, \dots, N$

For accessibility, we interpret the updating rules given in Equations (15)–(17) as follows:

1. The success of the flock's top performer inspires an individual to attempt to imitate its behavior. Stated differently, doves seek out more food by moving toward the one that is most satiated. The position vector w_j^e is updated to more precisely resemble the position vector of the dove with the greatest degree of satiety, $w_{d_s}^e$, to simulate this social learning. (i.e., $w_j^{e+1} = w_j^e + \eta \beta_j^e (w_{d_s}^e - w_j^e)$)

2. A dove is less likely has to modify its existing method of consuming and become more cautious when it is more satiated. A dove with a lower degree of satisfaction, on the other hand, is more inclined to imitate the behavior of the top performer and to want to alter its foraging strategy. The behavior is modified according to the amount of the first term on the right-hand side of equation (9) to simulate this social impact (i.e., $(\frac{s_{b_s}^e - s_j^e}{s_{b_s}^e})$).

3. In essence, the social influence diminishes as it spreads, indicating that the divide between the flock's best dove and the dove is negatively correlated with the impact. The quantity is modified proportionately to the third term's value on equation (9) right side to reflect this type of social impact (i.e., $(1 - \frac{\|w_j^e - w_{d_s}^e\|}{\max \text{Distance}})$)

To improve the performance of Dove Swarm Optimization (DSO), balancing exploration (global search) and exploitation (local search) is crucial. Exploration ensures The method can identify possibilities by efficiently searching the solution space, while exploitation focuses on refining solutions within those regions to identify the optimal point. Below are some modifications and strategies that can enhance this balance in DSO:

Adaptive Step Sizes

Adaptive step sizes dynamically adjust the movement of doves during the optimization process based on the search stage.

• Mechanism:

- **Early Stage (Exploration):** Larger step sizes let doves more efficiently investigate the worldwide search area.
- **Later Stage (Exploitation):** Smaller step sizes provide more precise modifications around promising areas.
- Adjust the step size using a decaying function, for example:

$$\text{Step size} = \alpha \cdot e^{-\beta \cdot t} \quad (21)$$

where α is the initial step size, β is the decay rate, and t is the current iteration.

The Dove Swarm Optimization method becomes more efficient, dependable, and successful across a broad variety of optimization situations by including variable step sizes, especially those needing a delicate balance between exploration and exploitation.

Inspired by dove foraging behavior, the program operates a methodical exploration and exploitation phase:

- Initialization: Doves are distributed in the fuzzy parameter space using a topologically ordered scheme.
- Fitness Evaluation: Each dove's configuration is evaluated using:
 $f(w) = \text{Power} - \alpha \cdot \text{Error} - \beta \cdot \text{Overshoot} - \gamma \cdot \text{Response Time}$
- Satiety Update: as per eqn (14).
- Position Update: where: as per eqn (17).
- Adaptive Step Size: as per eqn (21).
- Termination Criteria: The optimization halts when: it meets as per eqn (18).

To guarantee the FLC stays responsive and accurate across different environmental circumstances, ADSO always monitors and changes the fuzzy rule base and membership functions. This synergy between real-time fuzzy inference and adaptive optimization leads to superior MPPT performance.

IV. EXPERIMENTAL RESULTS

A commercial photovoltaic (PV) panel, a DC-DC boost converter, and a dSPACE DS1104 real-time control platform were used to create a thorough experimental configuration meant to assess the efficacy of the suggested fuzzy-ADSO MPPT controller. The test conditions were designed to replicate real-world operating environments under variable solar irradiance and temperature.

Hardware Setup:

- PV Panel: 200W monocrystalline module
- DC-DC Converter: Custom-designed boost converter rated at 250W
- dSPACE Controller: DS1104 board running in real-time with MATLAB/Simulink interface
- Irradiance Source: Variable-intensity halogen lamp for controlled testing

- Measurement Instruments: Tektronix digital oscilloscope, I-V tracer, NI DAQ modules

The Performance Metrics are the Tracking Efficiency (%), Steady-State Oscillation (Watts), Response Time (ms) and Overshoot (%).



Figure 6: Tracking Efficiency Comparison

Figure 6 shows the Tracking efficiency reflects how effectively an MPPT controller can determine the PV panel's maximum power performance under a range of environmental circumstances. From the results, the Incremental Conductance (IncCond) algorithm achieved a tracking efficiency of 94.37%, which is acceptable but limited by its fixed-step approach. The Fuzzy Logic Controller (FLC) demonstrated a modest improvement, achieving 96.02% due to its rule-based adaptability and capacity to handle nonlinear behavior. However, the proposed FLC enhanced with Adaptive Dove Swarm Optimization (FLC + ADSO) significantly outperformed both, attaining a tracking efficiency of 98.91%. This improvement is primarily due to ADSO's ability to continuously fine-tune fuzzy rules and membership functions in real-time, allowing the controller to quickly respond to irradiance and temperature fluctuations.

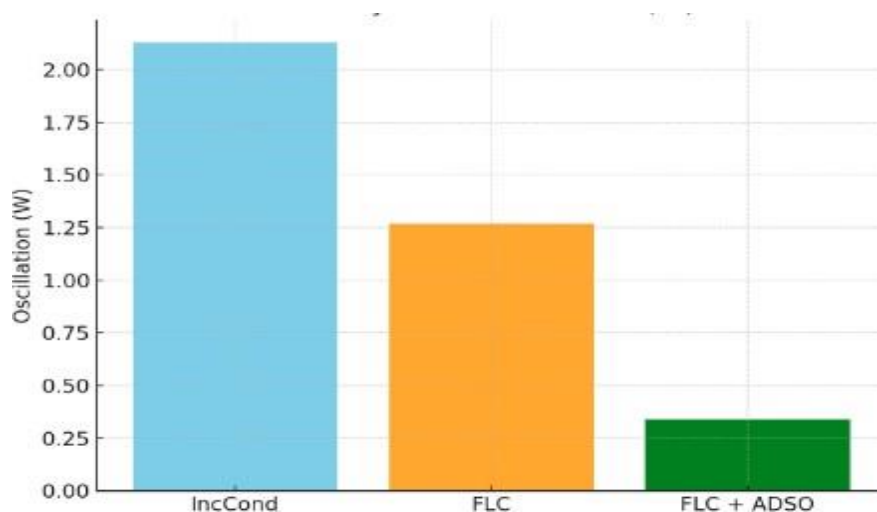


Figure 7: Steady-State Oscillation Comparison

Figure 7 shows the Steady-state oscillation represents the fluctuation of power output around the MPP during stable conditions. Larger oscillations result in reduced net power and may stress the power electronics. The IncCond method exhibited an oscillation amplitude of 2.13W, while the FLC reduced this to 1.27W by using smoother, rule-based control transitions. The FLC + ADSO approach showed a dramatic reduction to just 0.34W, indicating the controller's capability to maintain near-constant operation at the MPP. This performance gain confirms that ADSO effectively enhances the convergence behavior of the fuzzy system by intelligently regulating the step response and reducing fluctuation.



Figure 8: Response Time (ms) Comparison

Figure 8 show the Response time is critical in tracking the MPP efficiently, especially under dynamic environmental conditions. The slower the response, the more energy is lost during the transition. The IncCond method showed a delayed response of 412ms due to its sequential decision-making process. The FLC improved this with a 212ms response, leveraging rule-based logic. The FLC + ADSO controller delivered the fastest response at 112ms, showcasing its ability to rapidly adapt to environmental shifts. This reduced latency is attributed to ADSO's efficient optimization, which accelerates convergence toward the true MPP by actively learning and adjusting the fuzzy inference parameters.

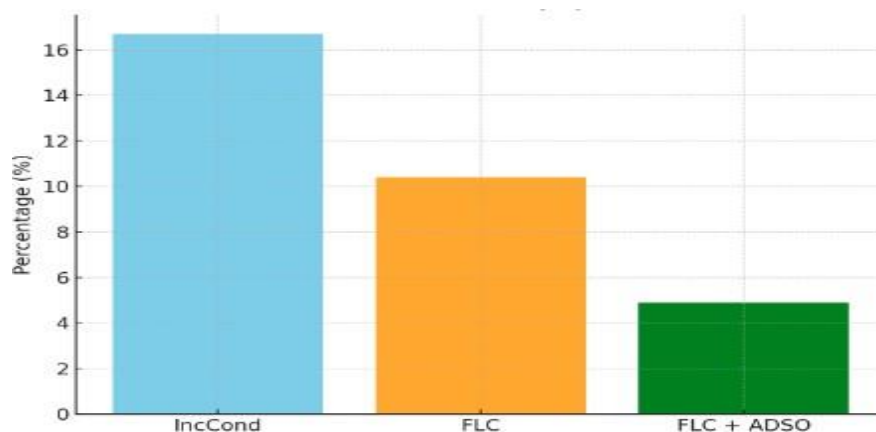


Figure 9: Overshoot Comparison

Figure 9 shows the Overshoot refers to the extent to which the system exceeds the MPP before stabilizing. A high overshoot may cause stress on system components and temporary inefficiencies. The IncCond controller exhibited a substantial overshoot of 16.7%, while the FLC improved this to 10.4%. With just 4.9% overshoot, the FLC + ADSO exhibited the most consistent behaviour. This emphasizes the capacity of the suggested hybrid controller to provide precise and effortless MPPT control. ADSO's incorporation provides precise control over dynamic changes, hence reducing forceful reactions usually resulting in overshooting.

V. CONCLUSION

A novel hybrid intelligent MPPT control technique combining a fuzzy logic controller (FLC) with Adaptive Dove Swarm Optimization (ADSO) for real-time power extraction from photovoltaic (PV) systems was offered in this research. A commercial PV module and a boost converter under dynamic irradiance circumstances were used to experimentally evaluate the suggested approach on a dSPACE DS1104 platform. Real-time modification of membership functions and rule sets was made possible by the combination of ADSO with fuzzy logic, hence greatly improving the tracking accuracy and rapid convergence of the MPPT controller. Compared results against conventional Incremental Conductance (IncCond) and solo FLC techniques showed the superiority of the proposed FLC-ADSO controller in terms of:

- Improved tracking efficiency (up to 98.91%)
- Reduced steady-state oscillation (0.34W)
- Faster response time (112 ms)
- Minimized overshoot (4.9%)

These performance gains validate the practical viability of using metaheuristic-enhanced fuzzy control for real-time MPPT in PV systems, especially in conditions with rapidly changing solar irradiance and temperature. The FLC-ADSO hybrid approach offers a scalable, model-free, and high-efficiency solution for modern renewable energy systems. Future directions include integrating this controller with energy storage systems, exploring grid-connected configurations, and implementing lightweight versions of the algorithm suitable for embedded platforms and IoT-based smart energy systems. Moreover, real-time wireless monitoring and cloud analytics could further improve the overall system's adaptability, diagnostics, and control.

REFERENCES

1. Lee, J.S.; Lee, K.B. Variable DC-link voltage algorithm with a wide range of maximum power point tracking for a two-string PV system. *Energies* 2013, 6, 58–78.
2. Shen, C.L.; Tsai, C.T. Double-linear approximation algorithm to achieve maximum-power-point tracking for photovoltaic arrays. *Energies* 2012, 5, 1982–1997.
3. Yau, H.T.; Wu, C.H. Comparison of extremum-seeking control techniques for maximum power point tracking in photovoltaic systems. *Energies* 2011, 4, 2180–2195.

4. Sera, D.; Kerekes, T.; Teodorescu, R.; Blaabjerg, F. Improved MPPT Algorithms for Rapidly Changing Environmental Conditions. In Proceedings of Power Electronics and Motion Control, Portoroz, Slovenia, 30 August–1 September 2006; pp. 1614–1619.
5. Chen, Y.T.; Lai, Z.H.; Liang, R.H. A novel auto-scaling variable step-size MPPT method for a PV system. *Sol. Energy* 2014, *102*, 247–256.
6. Radjaia, T.; Rahmania, L.; Mekhilefb, S.; Gaubertc, J.P. Implementation of a modified incremental conductance MPPT algorithm with direct control based on a fuzzy duty cycle change estimator using dSPACE. *Sol. Energy* 2014, *110*, 325–337.
7. Abdelsalam, A.K.; Massoud, A.M.; Ahmed, S.; Enjeti, P. High-Performance Adaptive Perturb and Observe MPPT Technique for Photovoltaic-Based Microgrids. *IEEE Trans. Power Electron.* 2011, *26*, 1010–1021.
8. Liu, F.; Duan, S.; Liu, F.; Liu, B.; Kang, Y. A Variable Step Size INC MPPT Method for PV Systems. *IEEE Trans. Ind. Electron.* 2008, *55*, 2622–2628.
9. Pandey, A.; Dasgupta, N.; Mukerjee, A.K. High-Performance Algorithms for Drift Avoidance and Fast Tracking in Solar MPPT System. *IEEE Trans. Energy Convers.* 2008, *23*, 681–689.
10. Mei, Q.; Shan, M.W.; Liu, L.Y.; Guerrero, J.M. A Novel Improved Variable Step-Size Incremental-Resistance MPPT Method for PV Systems. *IEEE Trans. Ind. Electron.* 2011, *58*, 2427–2434.
11. Messai, A.; Mellit, A.; MassiPavan, A.; Guessoum, A.; Mekki, H. FPGA-based implementation of a fuzzy controller (MPPT) for photovoltaic module. *Energy Convers. Manag.* **2011**, *52*, 2695–2704.
12. Jiang LL, Maskell DL, Patra JC. A novel ant colony optimization-based maximum power point tracking for photovoltaic systems under partially shaded conditions. *Energy and Buildings*. 2013 Mar 1; *58*:227-36.
13. Gros S, Quirynen R, Diehl M. An improved real-time economic NMPC scheme for Wind Turbine control using spline-interpolated aerodynamic coefficients. In 53rd IEEE Conference on Decision and Control 2014 Dec 15 (pp. 935-940). IEEE.
14. Liu YH, Huang SC, Huang JW, Liang WC. A particle swarm optimization-based maximum power point tracking algorithm for PV systems operating under partially shaded conditions. *IEEE transactions on energy conversion*. 2012 Oct 1; *27*(4):1027-35.
15. Ishaque K, Salam Z, Amjad M, Mekhilef S. An improved particle swarm optimization (PSO)-based MPPT for PV with reduced steady-state oscillation. *IEEE transactions on Power Electronics*. 2012 Jan 23; *27*(8):3627-38.
16. Iqbal A, Abu-Rub H, Ahmed SM. Adaptive neuro-fuzzy inference system based maximum power point tracking of a solar PV module. In 2010 IEEE International Energy Conference 2010 Dec 18 (pp. 51-56). IEEE.
17. Dzung PQ, Lee HH, Vu NT. The new MPPT algorithm using ANN-based PV. In International Forum on Strategic Technology 2010 2010 Oct 13 (pp. 402-407). IEEE.
18. Faranda R, Leva S. Energy comparison of MPPT techniques for PV Systems. *WSEAS transactions on power systems*. 2008 Jun 1; *3*(6):446-55.

19. Rahmani R, Seyedmahmoudian M, Mekhilef S, Yusof R. Implementation of fuzzy logic maximum power point tracking controller for photovoltaic system.
20. Faraji R, Rouholamini A, Naji HR, Fadaeinedjad R, Chavoshian MR. FPGA-based real time incremental conductance maximum power point tracking controller for photovoltaic systems. IET Power Electronics. 2014 May;7(5):1294-304.